




Dynamic partial (co)variance forecasting model

Zirong Chen & Yao Zhou

To cite this article: Zirong Chen & Yao Zhou (2024) Dynamic partial (co)variance forecasting model, Quantitative Finance, 24:5, 643-653, DOI: [10.1080/14697688.2024.2342896](https://doi.org/10.1080/14697688.2024.2342896)

To link to this article: <https://doi.org/10.1080/14697688.2024.2342896>



View supplementary material 



Published online: 07 May 2024.



Submit your article to this journal 



Article views: 167



View related articles 



View Crossmark data 

Dynamic partial (co)variance forecasting model

ZIRONG CHEN^{†‡} and YAO ZHOU^{*†}

[†]Department of Antai College of Economics and Management, Shanghai Jiao Tong University, Shanghai, People's Republic of China

[‡]The People's Bank of China, Beijing, People's Republic of China

(Received 18 May 2023; accepted 9 April 2024; published online 7 May 2024)

In this study, we propose a dynamic partial (co)variance forecasting model (DPCFM) by introducing a dynamic model averaging (DMA) approach into a partial (co)variance forecasting model. The dynamic partial (co)variance forecasting model considers the time-varying property of the model's parameters and optimal threshold combinations used to construct partial (co)variance. Our empirical results suggest that in both variance and covariance cases, the dynamic partial variance forecasting model can generate more accurate forecasts than an individual partial (co)variance forecasting model in both the statistical and economic sense. The superiority of the dynamic partial (co)variance forecasting model is robust to various forecast horizons.

Keywords: Partial (co)variance forecasting; Realized variance; Dynamic model averaging

JEL Classifications: C58, C22, G14, G13

1. Introduction

Variance, as a pivotal measure of risk, plays a crucial role in the realms of portfolio construction, asset allocation and risk management. The precise measure of variance has emerged as a hot topic of research in econometrics and finance. In the early stage, scholars usually use low-frequency data to forecast variance (Engle 1982, Bollerslev 1986). As the research in variance intensifies, Andersen and Bollerslev (1998) propose to use high-frequency data to forecast realized variance (RV). Due to the characteristics of unbiasedness, comprehensive information inclusion and robustness, RV gradually becomes the mainstream of variance measure (Andersen *et al.* 2010). Subsequently, the heterogeneous auto-regressive RV (HAR-RV) proposed by Corsi (2009) is the most popular one. Thereby, many following researches are extended based on the HAR-RV model (Andersen *et al.* 2007, Patton and Sheppard 2015).

As a further extension of the RV forecasting framework, Bollerslev *et al.* (2022) propose a realized partial-variance forecasting model by generalizing the realized semi-variance model introduced by Barndorff-Nielsen *et al.* (2008). This paper proves exceedingly challenging to outperform the zero-threshold or the semi-variance model when focusing exclusively on partial variances with a single threshold. However, this is not the case in the Chinese stock market, and figure 1

distinctly shows this divergent phenomenon. It shows the out-of-sample forecast mean standard errors (MSEs) associated with the Shanghai Composite Index (SSE index) based on rolling sample-estimation windows encompassing 500 observations. The data underpinning this study spans from January 1, 2013 to December 31, 2021. It is noting that this analysis particularly focuses on the impact of varying quantiles in the construction of partial variances.[†] Obviously, the pattern is not consistent. Subsamples 1 and 3 show analogous pattern, achieving their lowest MSEs at approximately 0.5 and 0.6, respectively. However, the whole sample displays a totally different pattern, and the partial variance with a 0.5 threshold quantile exhibits the poorest forecasting performance.

The discrepancy between figure 1 and findings in Bollerslev *et al.* (2022) underscores the impact of the selection of thresholds and sample periods on the predictive accuracy of RV. Such variability also highlights the instability of depending solely on a single partial variance forecasting model over time (Stock and Watson 2003, 2004). The time-varying nature of RV and the choice of thresholds motivate us the adoption of a dynamic method, aptly addressed by the Dynamic Averaging Method (DMA). Initially proposed by Raftery *et al.* (2010) and later introduced to economics by Koop and

[†] The sample data, comprising three random subsamples (January 1, 2013–June 30, 2016; July 1, 2016–June 30, 2019; and July 1, 2019–December 31, 2021), demonstrate the inconsistency in the predictive efficacy of realized partial variance forecasting. This inconsistency supports the research presented in this study.

*Corresponding author. Email: faunayao@sjtu.edu.cn

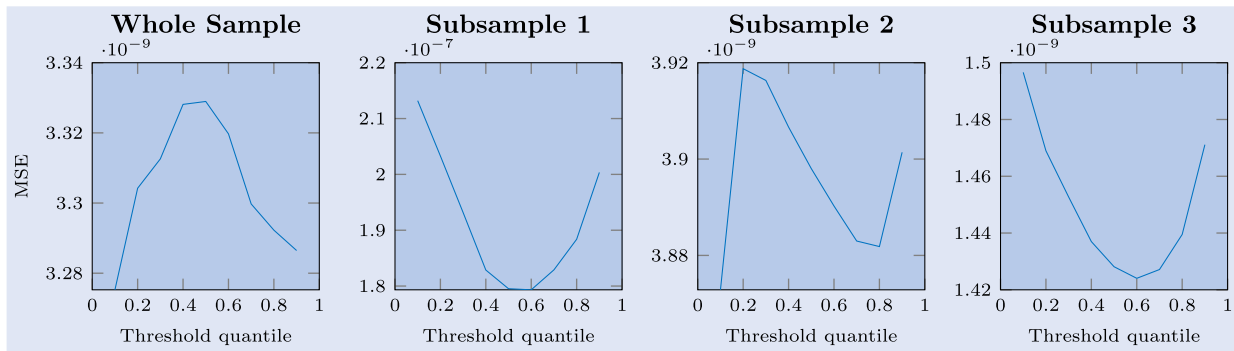


Figure 1. Out-of-sample performance of HAR-PV(1) in different sub-samples.

Korobilis (2012), DMA offers a suitable framework for this context. This article employs the DMA to combine forecasts of all of the partial variance forecasting models constructed from different threshold combinations. This approach allows for adaptable threshold combinations, enhancing both the certainty and accuracy of predictions. Consequently, the reliability of RV predictions is enhanced, reducing the sensitivity to specific thresholds and sample period choices.

This study contributes to the literature in three dimensions. First, the incorporation of the DMA method enables us to consider time variations in the parameters of variance models. Many studies (Calvet and Fisher 2004, Granger and Hyung 2004, Banerjee and Urga 2005) find that the statistical property of variance undergoes frequent structural breaks or switches between different regimes. Time-varying parameters in variance forecasting models enhance accuracy, thereby improving following forecast results. Second, the DMA can effectively model the time-varying variance of realized variance and combine different forecasting models. As Corsi *et al.* (2008) highlights that RV estimators, due to their time-varying variance, are susceptible to heteroskedastic errors, making the measurement of such variance vital for reducing uncertainty and enhancing predictive accuracy. Additionally, DMA's ability to combine various RV models mitigates inaccuracies inherent in single-model reliance (Stock and Watson 2003, 2004). Liu and Maheu (2009) demonstrate this by combining HAR-type model forecasts with constant-coefficient models using Bayesian model averaging. Similarly, Wang *et al.* (2016) apply DMA to merge forecasts from eight distinct HAR-type models, considering the time-varying nature of model parameters. We employ high-frequency (5-min interval) price data for the SSE index and 20 individual stocks in our forecasting analysis. The empirical results show that DMA forecasts are more accurate than most individual partial-variance forecasting models, indicating that predictive ability can be improved by allowing a model to change over time. Third, we extend the dynamic partial variance forecasting model to covariance. Using the model confidence set (MCS) test developed in Hansen *et al.* (2011), we compare forecasting methods from the two perspectives of predictive accuracy and economic value. We find empirical evidence that the DMA method can substantially improve predictive accuracy and that the improvement is robust to alternative forecast horizons and samples.

The remainder of the paper is organized as follows. In section 2, we briefly describe the partial-variance forecasting

model, DMA method and dynamic partial (co)variance forecasting model. In Section 3, we describe the data and conduct some preliminary analysis. In section 4, we report the main empirical finding regarding forecasting realized variance. In section 5, we provide the empirical results on forecasting realized covariance (RCOV). Last, section 6 concludes. The online Supplementary Appendix contains additional details and empirical results.

2. Econometric methodology

In this section, we first briefly describe the partial (co)variance forecasting model, then introduce the dynamic partial (co)variance forecasting model (DPCFM).

2.1. Partial (co)variance forecasting model

Suppose we have N assets, and $\mathbf{r}_{t,k} = [r_{t,k}^{(1)}, \dots, r_{t,k}^{(N)}]'$ denotes intra-daily return for all the assets. Then the RCOV matrix can be written as follows:

$$\mathbf{RCOV}_t = \sum_{k=1}^M \mathbf{r}_{t,k} \mathbf{r}_{t,k}' \quad (1)$$

Bollerslev *et al.* (2020) divide RCOV into three components: 'negative', 'positive', and 'mixed' semi-covariance matrices. Let $n(x) = \min\{x, 0\}$ and $p(x) = \max\{0, x\}$ denote the element-wise positive and negative components of the real vector. The three realized semi-covariance matrices are then given as follows:

$$\begin{aligned} \mathbf{N}_t &= \sum_{k=1}^M n(\mathbf{r}_{t,k}) n(\mathbf{r}_{t,k})', & \mathbf{P}_t &= \sum_{k=1}^M p(\mathbf{r}_{t,k}) p(\mathbf{r}_{t,k})', \\ \mathbf{M}_t &= \sum_{k=1}^M n(\mathbf{r}_{t,k}) p(\mathbf{r}_{t,k})' + p(\mathbf{r}_{t,k}) n(\mathbf{r}_{t,k})'. \end{aligned} \quad (2)$$

Bollerslev *et al.* (2022) generalize semi-covariances to partial covariances by considering the use of multiple thresholds rather than a single threshold at zero. In particular, suppose we have G thresholds that satisfy $\mathbf{c}_0 = -\infty$, $\mathbf{c}_{G+1} = +\infty$, and $\mathbf{c}_{g-1} < \mathbf{c}_g, \forall g$. Then, the realized partial covariance is defined

by

$$\mathbf{PCOV}_t^{(g,g')} = \sum_{k=1}^M f_g(\mathbf{r}_{t,k}) f_{g'}(\mathbf{r}_{t,k})'. \quad (3)$$

where $f_g = \mathbf{x} \circ \mathbb{I}\{\mathbf{c}_g < \mathbf{x} < \mathbf{c}_{g+1}\}$. Following Bollerslev *et al.* (2022), we combine all the ‘mixed’ partial covariance, ($g \neq g'$), and finally obtain $(G+1)(G+2)/2$ partial covariance matrices in total rather than G^2 .

In forecasting RCOV matrices, Chiriac and Voev (2011) propose the vech-HAR model. The scalar version of the vech-HAR model can be written as follows:

$$\begin{aligned} \text{vech}(\mathbf{RCOV}_{t+h|t+1}) &= \beta_0 + \beta_d \text{vech}(\mathbf{RCOV}_t) \\ &+ \beta_w \text{vech}(\mathbf{RCOV}_{t|t-4}) \\ &+ \beta_m \text{vech}(\mathbf{RCOV}_{t|t-21}) + \epsilon_t. \end{aligned} \quad (4)$$

where $\mathbf{RCOV}_{t+h|t} = \frac{1}{h+1} \sum_{i=1}^h \mathbf{RCOV}_{t+i}$, β_0 is an $N(N+1)/2$ vector, and β_d , β_w , and β_m are scalars.

The vech-HAR-RS and vech-HAR-PCOV(G) models can be written as follows:

$$\begin{aligned} \text{vech}(\mathbf{RCOV}_{t+h|t+1}) &= \beta_0 + \beta_d^N \text{vech}(\mathbf{N}_t) + \beta_d^M \text{vech}(\mathbf{M}_t) \\ &+ \beta_d^P \text{vech}(\mathbf{P}_t) + \beta_w \text{vech}(\mathbf{RCOV}_{t|t-4}) \\ &+ \beta_m \text{vech}(\mathbf{RCOV}_{t|t-21}) + \epsilon_t. \\ \text{vech}(\mathbf{RCOV}_{t+h|t+1}) &= \beta_0 + \sum_{g=1}^G \sum_{g'=g}^G \beta_d^{(g,g')} \text{vech}(\overline{\mathbf{PCOV}}_t^{(g,g')}) \\ &+ \beta_w \text{vech}(\mathbf{RCOV}_{t|t-4}) \\ &+ \beta_m \text{vech}(\mathbf{RCOV}_{t|t-21}) + \epsilon_t. \end{aligned} \quad (5)$$

where

$$\overline{\mathbf{PCOV}}_t^{(g,g')} = \begin{cases} \mathbf{PCOV}_t^{(g,g')}, & \text{for } g = g' \\ \mathbf{PCOV}_t^{(g,g')} + \mathbf{PCOV}_t^{(g',g)}. & \text{for } g \neq g' \end{cases} \quad (6)$$

Note that when the cross-sectional dimension is one, the $G(G+1)/2$ ‘mixed’ partial covariance terms reduce to zero and we have only $G+1$ realized partial variance:

$$RV_t = \sum_{g=1}^G PV_t(g). \quad (7)$$

where $PV_t(g) = \sum_{k=1}^M r_{k,t}^2 \mathbb{I}\{c_g < r_{k,t} \leq c_{g+1}\}$, for $g = 0, \dots, G$. Similarly, the HAR, HAR-RS and the partial variance forecasting model (HAR-PV(G)) can be written as follows:

$$\begin{aligned} RV_{t+h|t+1} &= \beta_0 + \beta_d RV_t + \beta_w RV_{t|t-4} + \beta_m RV_{t|t-21} + \epsilon_t, \\ RV_{t+h|t+1} &= \beta_0 + \beta_d^+ RS_t^+ + \beta_d^- RS_t^- + \beta_w RV_{t|t-4} \\ &+ \beta_m RV_{t|t-21} + \epsilon_t, \\ RV_{t+h|t+1} &= \beta_0 + \sum_{g=0}^G \beta_g PV_t(g) + \beta_w RV_{t|t-4} \\ &+ \beta_m RV_{t|t-21} + \epsilon_t. \end{aligned} \quad (8)$$

where $RS_t^+ = \sum_{k=1}^M r_{k,t}^2 \mathbb{I}\{r_{k,t} > 0\}$, $RS_t^- = \sum_{k=1}^M r_{k,t}^2 \mathbb{I}\{r_{k,t} < 0\}$, G represents the number of thresholds.

2.2. Dynamic partial (co)variance forecasting model

From equation (5), we know that it is crucial for a partial (co)variance forecasting model to choose the suitable number and location of thresholds. Bollerslev *et al.* (2022) relies on K-fold algorithms rooted in regression trees to determine the number and location of thresholds. However, the K-fold algorithm is computationally infeasible, especially when there are too many threshold combinations. In this context, we adopt the dynamic model averaging (DMA) approach to combine the forecast values from all the different partial (co)variance forecasting model, and propose the dynamic partial (co)variance forecasting model (DPCFM). The DMA approach allows not only regression coefficients but also the entire forecasting model to change over time. Here, we first briefly introduce the DMA method.

Suppose we have K numbers of models, each of which takes a different set of predictors. These TVP models can be written as follows:

$$y_t = x_t^{(k')} \beta_t^{(k)} + \epsilon_t^{(k)}, \quad \beta_t^{(k)} = \beta_t^{(k)} + \eta_t^{(k)}. \quad (9)$$

where y_t is the dependent variable to forecast, the vector $x_t^{(k)}$ is the set of predictors for model k including the intercept, and the vector $\beta_t^{(k)}$ represents the time-varying coefficients; $\epsilon_t^{(k)} \sim N(0, H_t)$, $\eta_t^{(k)} \sim N(0, Q_t)$. $\epsilon_t^{(k)}$ and $\eta_t^{(k)}$ are assumed to be mutually independent at all of the leads and lags, and $k = 1, \dots, K$.

First, we need to use the Kalman filter to estimate and forecast y_t for each model k . Starting at $t=0$, Kalman filtering updates these formulae and makes a prediction based on the following predictive distribution:

$$y_t | y_{t-1} \sim N(x_{t-1} \beta_{t|t-1}^{(k)}, H_t^{(k)} + x_{t-1} \Sigma_{t|t-1}^{(k)} x_{t-1}^{(k')}). \quad (10)$$

where $\beta_{t|t-1}^{(k)} = \beta_{t|t}^{(k)}$ and $\Sigma_{t|t-1}^{(k)} = \Sigma_{t-1|t-1}^{(k)} + Q_t^{(k)}$.

The Kalman filter relies on the following two equations to estimate and forecast y_t :

$$\begin{aligned} \beta_{t|t}^{(k)} &= \beta_{t|t-1}^{(k)} + \Sigma_{t|t-1}^{(k)} x_t^{(k')} (H_t^{(k)} + x_{t-1}^{(k')} \Sigma_{t|t-1}^{(k)} x_{t-1}^{(k)})^{-1} \\ &\times (y_t - x_{t-1}^{(k')} \beta_{t|t-1}^{(k)}), \\ \Sigma_{t|t}^{(k)} &= \Sigma_{t|t-1}^{(k)} - \Sigma_{t|t-1}^{(k)} x_t^{(k')} (H_t^{(k)} + x_{t-1}^{(k')} \Sigma_{t|t-1}^{(k)} x_{t-1}^{(k)})^{-1} \\ &\times x_{t-1}^{(k')} \Sigma_{t|t-1}^{(k)}. \end{aligned} \quad (11)$$

where $\Sigma_{t|t-1}^{(k)}$ is the covariance matrix of $\beta_{t|t-1}^{(k)}$. Additional details can be found in Kim and Nelson (1999).

Following Raftery *et al.* (2010) and Koop and Korobilis (2012), we estimate two covariance matrices as follows:

$$\begin{aligned} Q_t^{(k)} &= \left(\frac{1}{\lambda} - 1 \right) \Sigma_{t-1|t-1}^{(k)}, \\ \hat{H}_t^{(k)} &= \frac{1 - \kappa}{1 - \kappa^{t-1}} \sum_{j=1}^{t-1} \kappa^j (y_{t-j} - x_{t-j-1}^{(k)} \beta_{t-j|t-j-1}^{(k)})^2. \end{aligned} \quad (12)$$

where $0 \leq \lambda \leq 1$ is referred to as a forgetting factor, κ is the decay factor.

Having obtained a forecast value, we must determine the model probability for model k , we use $\pi_{t|t-1,k}$ to denote the probability for model k . Raftery *et al.* (2010) define the probability for model k as follows:

$$\pi_{t|t-1,k} = \frac{\pi_{t-1|t-1,k}^\alpha}{\sum_{k=1}^K \pi_{t-1|t-1,k}^\alpha}. \quad (13)$$

where $0 \leq \alpha \leq 1$ is another forgetting factor, which avoids specifying a large transition probability matrix and thus results in a substantial computational gain. We perform a simpler evaluation by updating the equation as follows:

$$\pi_{t|t,k} = \frac{\pi_{t|t-1,k} p_k(y_t | \mathcal{F}_{t-1})}{\sum_{k=1}^K \pi_{t|t-1,k} p_k(y_t | \mathcal{F}_{t-1})}. \quad (14)$$

where $p_k(y_t | \mathcal{F}_{t-1})$ represents the predictive density for model k . Having obtained a forecast value and a probability for each model k at day t , the DMA computes the average of K forecasts by using probabilities as model weights, while the DMS chooses a specific model with the maximum probability at each time point. Therefore, the DMA and DMS forecasts can respectively be computed as follows:

$$\hat{y}_t^{DMA} = \sum_{k=1}^K \pi_{t|t-1,k} \hat{y}_{t|t-1}^{(k)}, \quad \hat{y}_t^{DMS} = \hat{y}_{t|t-1}^{(k^*)}. \quad (15)$$

where k^* indexes the model with the highest probability.

The dynamic (co)variance forecasting model (DPCFM) use the DMA approach to combine the forecast results from different partial (co)variance forecasting model. When applying the DMA approach, we need to preselect certain threshold combinations and establish a corresponding partial (co)variance forecasting model. Given the large movements in return variance over time, we use the time-varying,

asset-specific quantiles of the variance standardized return distribution as thresholds. Specifically,

$$c_{t,g} = RV_t^{1/2} Q\left(\frac{r_{tj}}{RV_t^{1/2}}; q_g\right), \quad g = 2, \dots, G \quad (16)$$

where $Q(z; q_g)$ denotes the sample q_g quantile of z . In this paper, The grid of quantiles ranges from 0.1 to 0.9 in increments of 10%, thus we have 9, 36, 84, and 126 different HAR-PCOV(1), HAR-PCOV(2), HAR-PCOV(3), and HAR-PCOV(4) models respectively.

3. Data

In this study, we use the Shanghai Composite Index (SSE) as our main research object. The sample period ranges from January 1, 2013 to December 31, 2021, covering 2188 trading days. To avoid the effect of micro-structure noise, the sampling frequency is set to be 5 min.

In order to explore the predictive ability of the DMA model in forecasting realized covariance matrices, we select 20 individual stocks with continuous trading history and less than 10 limit-up trading days during the sample period. The selected stocks can be found in table 1.

Table 2 reports the descriptive statistics of different realized measures, where $PV_{t,[0,0.1]}^{(1)}$ and $PV_{t,[0.9,1]}^{(1)}$ represent the partial variances during quantiles $[0, 0.1]$ and $[0.9, 1]$, respectively, while J_t only reports the summary statistics for the positive part. We report the medians for all the 20 individual stocks. Clearly, all the realized measures are highly skewed and all display positive kurtosis, suggesting that they have non-Gaussian distributions. From a comparison, we find that the individual stocks are more volatile than the SSE index.

Table 1. Selected individual stock.

Stock Code	Stock Name	Industry
000869.SZ	Yantai Changyu Pioneer Wine Company Limited	Beverages–Wineries & Distilleries
000919.SZ	Jinling Pharmaceutical Company Limited	Drug Manufacturers–Specialty & Generic
002294.SZ	Shenzhen Salubris Pharmaceuticals Co., Ltd.	Medical Instruments & Supplies
002304.SZ	Jiangsu Yanghe Brewery Joint-Stock Co., Ltd.	Beverages–Wineries & Distilleries
002393.SZ	Tianjin Lisheng Pharmaceutical Co., Ltd.	Drug Manufacturers–Specialty & Generic
002394.SZ	Jiangsu Lianfa Textile Co., Ltd.	Textile Manufacturing
600007.SS	China World Trade Center Co., Ltd.	Real Estate Services
600011.SS	Huaneng Power International, Inc.	Utilities–Independent Power Producers
600016.SS	China Minsheng Banking Corp., Ltd.	Banks–Regional
600377.SS	Jiangsu Expressway Company Limited	Infrastructure Operations
600456.SS	Baoji Titanium Industry Co., Ltd.	Other Industrial Metals & Mining
600563.SS	Xiamen Faratronic Co., Ltd.	Electronic Components
600600.SS	Tsingtao Brewery Company Limited	Beverages–Brewers
600660.SS	Fuyao Glass Industry Group Co., Ltd.	Auto Parts
600971.SS	Anhui Hengyuan Coal-Electricity Group Co., Ltd.	Thermal Coal
601098.SS	China South Publishing & Media Group Co., Ltd.	Publishing
601601.SS	China Pacific Insurance (Group) Co., Ltd.	Insurance–Life
601607.SS	Shanghai Pharmaceuticals Holding Co., Ltd.	Medical Distribution
601808.SS	China Oilfield Services Limited	Oil & Gas Equipment & Services
601898.SS	China Coal Energy Company Limited	Thermal Coal

Table 2. Descriptive statistics of realized variances.

	RV_t	CV_t	J_t	RS_t^+	RS_t^-	$PV_{t,[0,0.1]}^{(1)}$	$PV_{t,[0.9,1]}^{(1)}$
SSE Index							
Mean $\times 10^4$	1.246	1.152	0.384	0.624	0.623	0.437	0.429
Median $\times 10^4$	0.557	0.497	0.167	0.282	0.253	0.170	0.192
Maximum $\times 10^4$	40.434	43.229	5.991	27.654	20.636	16.117	20.937
Minimum $\times 10^4$	0.067	0.047	0.020	0.024	0.019	0.015	0.014
Std.Dev. $\times 10^4$	2.749	2.662	0.695	1.425	1.454	1.047	1.059
Skewness	7.847	8.243	5.062	9.067	7.491	7.542	9.697
Kurtosis	84.947	92.815	34.271	117.601	77.169	78.261	130.369
Individual Stock							
Mean $\times 10^4$	5.156	4.477	1.898	2.767	2.390	1.765	2.143
Median $\times 10^4$	2.895	2.455	0.978	1.463	1.304	0.911	1.056
Maximum $\times 10^4$	114.891	102.897	45.812	67.644	68.327	54.209	62.383
Minimum $\times 10^4$	0.217	0.134	0.089	0.063	0.061	0.044	0.029
Std.Dev. $\times 10^4$	7.442	6.633	3.751	4.187	3.839	3.018	3.471
Skewness	6.697	6.564	6.736	5.946	7.817	7.796	6.098
Kurtosis	72.469	72.118	66.913	55.047	93.811	96.463	56.088

Notes: This table reports the summary statistics of different realized measures. $PV_{t,[0,0.1]}^{(1)}$ and $PV_{t,[0.9,1]}^{(1)}$ represents the partial variance during quantile [0, 0.1] and [0.9, 1] respectively. J_t only reports the summary statistic of the positive part. For individual stocks, we report the median of all the 20 individual stocks.

4. Forecasting realized variance

4.1. In-sample analysis

This subsection provides the in-sample estimation for several specific partial variance forecasting models with different threshold combinations based on the SSE index. Following the choice of threshold combination in Bollerslev *et al.* (2022), the threshold quantile is set to be 0.9 for the single-threshold partial variance model, because many studies (see e.g. Bollerslev *et al.* 2022) find that large positive returns have a great effect on forecasting realized variance. When the threshold number equals 2, we select one low and one high threshold ($\{0.2, 0.8\}$), so that we can investigate how the abnormal return affects the future realized variance. Furthermore, we select the median and two tail thresholds in the three-threshold model ($\{0.2, 0.5, 0.8\}$), and thus the leverage effects can be considered. Last, the four-threshold model divides the positive returns more precisely ($\{0.2, 0.5, 0.7, 0.9\}$). Besides, we conduct sub-sample analysis to avoid the impact of sample selection, and the entire sample is randomly divided into two sub-samples. The first sub-sample spans from January 1, 2013 to June 30, 2016 (period 1), while the second sub-sample covers the period from July 1, 2016 to December 31, 2021 (period 2).

Table 3 reports the correlation matrix between different partial variance. The column labeled ‘VIF’ reports the Variance Inflation Factor of each variable. Firstly, from the correlation coefficient matrix, it is evident that there are high correlations between various partial variances, indicating the possible presence of multicollinearity. Subsequently, we conducted VIF tests on the model, revealing that the VIF for $PV_t^{(4)}$ in HAR-PV(4) is as high as 16. This finding suggests that we might need to consider the impact of multicollinearity.

To address the issue of multicollinearity, we consider using ridge regression to estimate the partial variance model. We report the ridge regression results in table 4, the coefficient ‘ k ’ in ridge regression was selected using cross-validation, aiming to minimize the estimation error. Because the average values of the partial variances may differ greatly, we standardize all right-hand side variables to be mean zero and variance one, such that we can directly compare all the coefficients. From the estimation based on the entire sample, several observations can be made: First, the parameter estimates of weekly and monthly RV in each model are all significant at the 1% level, suggesting strong persistence in the RV dynamics. Second, the partial variance around zero is more significant than the tail partial variance in forecasting next-day realized variance. These results are found in the four partial-variance forecasting models. For example, in the estimation result for

Table 3. Correlation table.

		$PV_t^{(1)}$	$PV_t^{(2)}$	$PV_t^{(3)}$	$PV_t^{(4)}$	$PV_t^{(5)}$	VIF
HAR-PV(4)	$PV_t^{(1)}$	1.000	0.834	0.650	0.830	0.798	5.236
	$PV_t^{(2)}$		1.000	0.450	0.719	0.719	4.254
	$PV_t^{(3)}$			1.000	0.868	0.714	5.884
	$PV_t^{(4)}$				1.000	0.901	16.502
	$PV_t^{(5)}$					1.000	6.162

Notes: This table reports the correlation between different partial variance in HAR-PV(4) model. The choice of thresholds for HAR-PV(4) is $\{0.2, 0.5, 0.7, 0.9\}$.

Table 4. In-sample analysis of SSE index.

		$PV_t^{(1)}$	$PV_t^{(2)}$	$PV_t^{(3)}$	$PV_t^{(4)}$	$PV_t^{(5)}$	$RV_{t t-4}$	$RV_{t t-21}$	Ridge k value
All Sample	HAR-PV(1)	0.529*** (18.859)	-0.155*** (-5.601)				0.364*** (15.554)	0.080*** (4.159)	0.002
	HAR-PV(2)	0.208*** (6.793)	0.513*** (13.374)	-0.307*** (-10.224)			0.350*** (15.409)	0.065*** (3.500)	0.002
	HAR-PV(3)	0.131*** (4.413)	0.484*** (19.245)	-0.016 (-0.605)	-0.143*** (-4.626)		0.334*** (15.427)	0.105*** (5.877)	0.003
	HAR-PV(4)	0.140*** (4.772)	0.559*** (21.120)	0.210*** (6.731)	-0.436*** (-8.361)	0.023 (0.735)	0.340*** (15.919)	0.111*** (6.291)	0.002
Sub-sample 1	HAR-PV(1)	0.539*** (11.718)	-0.170*** (-3.713)				0.365*** (9.635)	0.077** (2.429)	0.005
	HAR-PV(2)	0.220*** (4.387)	0.521*** (8.242)	-0.330*** (-6.644)			0.353*** (9.629)	0.063** (2.065)	0.005
	HAR-PV(3)	0.139*** (2.873)	0.499*** (12.170)	-0.035 (-0.799)	-0.150*** (-2.948)		0.330*** (9.499)	0.102*** (3.479)	0.007
	HAR-PV(4)	0.143*** (2.999)	0.579*** (13.278)	0.200*** (3.825)	-0.442*** (-5.083)	0.015 (0.290)	0.336*** (9.809)	0.108*** (3.711)	0.004
Sub-sample 2	HAR-PV(1)	0.290*** (8.689)	0.083*** (3.055)				0.317*** (9.953)	0.029 (0.983)	0.011
	HAR-PV(2)	0.006 (0.154)	0.399*** (10.063)	0.024 (0.823)			0.254*** (8.004)	0.004 (0.148)	0.009
	HAR-PV(3)	-0.041 (-1.101)	0.310*** (11.149)	0.117*** (4.222)	0.073** (2.330)		0.264*** (8.357)	0.005 (0.172)	0.011
	HAR-PV(4)	-0.016 (-0.427)	0.330*** (11.933)	0.174*** (6.237)	-0.134*** (-2.664)	0.104*** (3.618)	0.275*** (8.743)	0.007 (0.235)	0.009

Notes: This table reports the in-sample analysis of the SSE index at three different sub-samples. The whole sample covers the period from 2013.1.1 to 2021.12.31, the first sub-sample covers the period from 2013.1.1 to 2016.6.30, the second sub-sample covers the period from 2016.7.1 to 2021.12.31. ***, **, * indicates the significance at the 1%, 5%, 10% two-tail level respectively. The selected threshold combinations for HAR-PV(1), HAR-PV(2), HAR-PV(3), HAR-PV(4) are {0.9}, {0.2,0.8}, {0.2,0.5,0.8} and {0.2,0.5,0.7,0.9} respectively.

HAR-PV(4), the t -statistics for $PV_t^{(1)}$ and $PV_t^{(5)}$ are 4.772 and 0.735, respectively; while, the t -statistic for $PV_t^{(2)}$ equals 21.120, significant at the 1% level. Obviously, the significance of $PV_t^{(2)}$ is more significant than that of tail partial variance.

Next, if we compare the estimation results in three different estimation periods, we can find some consistent patterns in the predictive ability of realized measures. For example, some persistent behavior can be seen in the significant parameter estimates of lagged weekly, and monthly volatilities. Despite the consistent patterns, the values, significance, and even the sign of the parameters in the three periods are not consistent. For example, the coefficient at $PV_t^{(3)}$ in HAR-PV(2) is significant and negative for the entire sample and sub-sample 1, whereas it is nonsignificant and positive for sub-sample 2. The inconsistent pattern can also be found in $PV_t^{(5)}$, whose coefficients are non-significant for the entire sample and sub-sample 1 but significant and positive for sub-sample 2.

Overall, our subsample analysis shows that the regression coefficients of partial variance vary with the sample period, or its predictive ability changes over time. This finding shows that it is more appropriate to use a TVP model in forecasting future realized variance.

4.2. Out-of-sample performance

In this subsection, we investigate the forecasting performance of different variance forecasting models. To further investigate how well the DPCFM performs in forecasting realized

variance, we also consider some alternative strategies, including mean forecast, trimmed mean, and discounted mean combinations. Specifically, we compare the forecasting accuracy of the strategies shown in table 5.

All of the forecasts for each model in this subsection are generated using recursive regressions. The initial in-sample data for parameter estimation contain the first 1000 observations. To quantitatively evaluate the forecasting accuracy, we use the MSE as loss function[†]:

$$MSE = \frac{1}{n} \sum_{i=1}^n (RV_i - \hat{RV}_i)^2, \quad (17)$$

where RV_t is the actual realized variance, \hat{RV}_t is the forecast value of realized variance, and n is the number of forecasts.

Table 6 reports the 12 shown strategies' forecasting performances. The row labeled with 'MSE' reports the MSE value, the row labeled 'p.val $dm_{CompareModel}$ ' reports the results of Diebold and Mariano (1995) tests between *CompareModel* and the remaining models, and the row labeled with 'p-val MCS' reports the p -values of 90% Model Confidence Set(MCS) of Hansen *et al.* (2011).[‡] Some interesting results may be observed. First, the DMA (0.99) model's forecasts

[†] In addition to the MSE loss function, We also present the results based on MSD and QLIKE loss function in supplementary material.

[‡] We use the confidence level of 90%, which allows us to exclude a model with a p -value smaller than 0.1. In other words, the forecasts of this model are significantly less accurate than other models in MCS. In this study, we use the SQ statistic to calculate the MCS p -value through 100000 stationary bootstraps with a block length of 25.

Table 5. Forecasting strategies.

Strategy Name	Detailed Strategy
Rolling HAR(HAR)	Rolling OLS forecasts using the HAR model. Rolling window is 1000 trading days.
Rolling 5-fold CV(CV)	Following Bollerslev <i>et al.</i> (2022), we select the threshold (combination of thresholds) as the quantiles that minimize the average MSE over the CV folds. Rolling windows of 1000 observations and a 5-fold CV are used.
DMA(0.99)	DPCFM base on DMA method with parameter of $\lambda = \alpha = 0.99$.
DMS(0.99)	DPCFM base on DMS method with parameter of $\lambda = \alpha = 0.99$.
DMA(0.95)	DPCFM base on DMA method with parameter of $\lambda = \alpha = 0.95$.
DMS(0.95)	DPCFM base on DMS method with parameter of $\lambda = \alpha = 0.95$.
BMA	DPCFM based on DMA method with parameter of $\lambda = \alpha = 1$.
BMS	DPCFM based on DMS method with parameter of $\lambda = \alpha = 1$.
Mean Combination (MC)	Equal-weighted average of forecasts from individual models with MC imposed on recursive forecasts from different partial variance models.
Trimmed Mean Combination (TMC)	TMC differs from MC by using forecasts after excluding the largest and smallest forecasts.
Discount Mean Square Prediction Error (DMSPE(δ))	It is also the weighted average of individual forecasts with DMSPE imposed on recursive forecasts from different partial variance model. The weight is k on day t defined as: $w_{k,t} = \frac{\phi_{k,t}^{-1}}{\sum_{i=1}^k \phi_{i,t}^{-1}}$, where $\phi_{k,t} = \delta^{t-s} \sum_{s=1}^t (RV_t - RV_s)^2$. The parameter δ is the discount factor. We consider $\delta = 1.0$ and $\delta = 0.9$, and we denote these DMSPE strategies by DMSPE(δ)

have the lowest MSE value among the 12 models, indicating a superior forecasting performance. From the DM test results, we know that the predictive ability of the DMA model is significantly superior to the traditional combination approach. However, when compared with the HAR model, the improvement of the DMA(0.99) model lacks statistical significance. In order to better compare the predictive ability of DMA(0.99) and HAR model, we also do the MCS test. DMA(0.99) model is always included in the MCS test, which means that it DMA(0.99) has the significantly better out-of-sample performance.

Second, the MCS p -values for the traditional combination approach are mostly less than 0.1, which means that the forecasting models that are based on the traditional combination approach are not in the MCS. This indicates that the traditional combination approach cannot capture the dynamic characteristic of variance, and thus the out-of-sample performance is poor.

Third, except for the DMA(0.99), the Rolling HAR and BMA models perform well. However, different from the results in Bollerslev *et al.* (2022), the Rolling 5-fold HAR model cannot outperform the traditional Rolling HAR model.

Table 6. Forecasting performance of DMA and alternative strategies over SSE index.

	HAR	CV	MC	TMC	DMSPE (0.9)	DMSPE (1.0)	BMA	BMS	DMS (0.95)	DMA (0.95)	DMS (0.99)	DMA (0.99)
MSE $\times 10^8$	0.325	0.354	0.441	0.442	0.442	0.441	0.318	0.322	0.458	0.436	0.328	0.317
p -val dm_{HAR}		0.930	0.966	0.966	0.966	0.965	0.358	0.511	0.984	0.983	0.325	0.190
p -val dm_{CV}			0.830	0.831	0.832	0.828	0.029	0.048	0.926	0.905	0.023	0.010
p -val dm_{MC}				0.501	0.876	0.110	0.028	0.035	0.930	0.816	0.012	0.010
p -val dm_{TMC}					0.829	0.114	0.028	0.034	0.930	0.817	0.012	0.010
p -val $dm_{DMSPE(0.9)}$						0.070	0.028	0.034	0.929	0.809	0.012	0.010
p -val $dm_{DMSPE(1.0)}$							0.029	0.035	0.932	0.824	0.013	0.010
p -val dm_{BMA}								0.987	0.987	0.990	0.441	0.237
p -val dm_{BMS}								0.984	0.987	0.987	0.296	0.130
p -val $dm_{DMS(0.95)}$										0.152	0.007	0.006
p -val $dm_{DMA(0.95)}$											0.004	0.003
p -val $dm_{DMS(0.99)}$												0.140
p -val MCS	(0.457)	(0.169)	(0.045)	(0.040)	(0.057)	(0.085)	(0.840)	(0.457)	(0.036)	(0.038)	(0.457)	(1.000)

Notes: This table provides the forecasting performance of DPCFM and its competing strategies. The number in bold denotes that the corresponding model has the lowest loss function under a specific criterion.

A possible reason for this result is that the Chinese stock market is more volatile than the US one, and thus models selected based on historical data may be inappropriate for forecasting future realized variance.

Based on the out-of-sample performance, we find that DPCFM performs well in forecasting realized variance. Because DPCFM can track the sources of uncertainty regarding the prediction, we use Dangel and Halling (2012)'s methodology by decomposing the prediction variance into three components:

$$\begin{aligned} \text{Var}(\hat{R}V_{t+1}) = & \sum_{n=1}^k \hat{V}_t \pi_{t+1|t,n} + \sum_{n=1}^k (Z_t^{(n)} \Sigma_{t+1|t} Z_t^{(n)'}) \pi_{t+1|t,n} \\ & + \sum_{n=1}^k (\hat{y}_{t+1|t,n} - \hat{y}_{t+1|t})^2 \pi_{t+1|t,n} \end{aligned} \quad (18)$$

where $\sum_{n=1}^k \hat{V}_t \pi_{t+1|t,n}$ is the expected observational variance, $\sum_{n=1}^k (Z_t^{(n)} \Sigma_{t+1|t} Z_t^{(n)'}) \pi_{t+1|t,n}$ is the expected variance from errors in estimating parameters and it is always referred to as the estimation uncertainty. $\sum_{n=1}^k (\hat{y}_{t+1|t,n} - \hat{y}_{t+1|t})^2 \pi_{t+1|t,n}$ characterizes model uncertainty with respect to variable selection and the time variation of regression coefficients.

Figure 2 plots the relative weights of three components of the SSE index's prediction variance based on DMA(0.99). Similar to the findings in Wang *et al.* (2016), the observation variance is the dominant source of the prediction variance. Moreover, the figure highlights the importance of considering the time variation of parameter, as the estimation parameter's uncertainty captures a major fraction of the remaining variance. However, we find that the model's uncertainty plays a more important role in a turbulent market. For example, the model's uncertainty is much higher than estimation uncertainty in the 2018 market crash.

4.3. Forecast horizon

After considering the predictive accuracy, this subsection explores the out-of-sample performance in forecasting realized variance over a longer horizon. We consider three

different forecast horizons: a week (5 days), two weeks (10 days), and a month (22 days).

Table 7 presents different models' out-of-sample performance when the forecast horizons are 5, 10, and 22 trading days. First, we can see that the DPCFM performs the best. In all three forecast horizons, the model with the lowest loss values is all DPCFM, while the corresponding MCS p -values are all 1. This result shows that the DPCFM has the strongest predictive power in all three forecast periods.

Second, we can find that the optimal parameter of DPCFM changes. When the forecast period is 10 or 22 days, the DMA(0.95) is the optimal, while for 1-day and 5-day prediction periods, the DMA(0.99) is the optimal. This is very easy to understand: the smaller the λ and α parameters, the more rapidly the model changes, and the more necessary for DPCFM to update the model according to the data. When the forecast period is long, the model persistence decreases; thus, we must change the model more frequently.

5. Forecasting realized covariance matrices

5.1. Forecasting covariance matrix

In this subsection, we focus on forecasting covariance matrices. Because it is extremely difficult to directly apply the DMA method to the vech-HAR model, we separately forecast every element in a covariance matrix. We first decompose the RCOV into partial covariances, and then forecast each element of the covariance matrix through the DMA method. To avoid errors in transforming the covariance matrix into a positive definite matrix, we use the RMSE loss function to compare different covariance forecasting model:

$$\text{RMSE} = \frac{1}{T} \sum_{t=1}^T \|E_t\|_F = \frac{1}{T} \sum_{t=1}^T \left[\sum_{i=1}^N \sum_{j=1}^N e_{ij,t}^2 \right]^{1/2}. \quad (19)$$

where $E_t = \widehat{\text{RCOV}}_t - \text{RCOV}_t$ is the difference between the forecast covariance matrix and the true covariance matrix. T is the total number of forecast days.

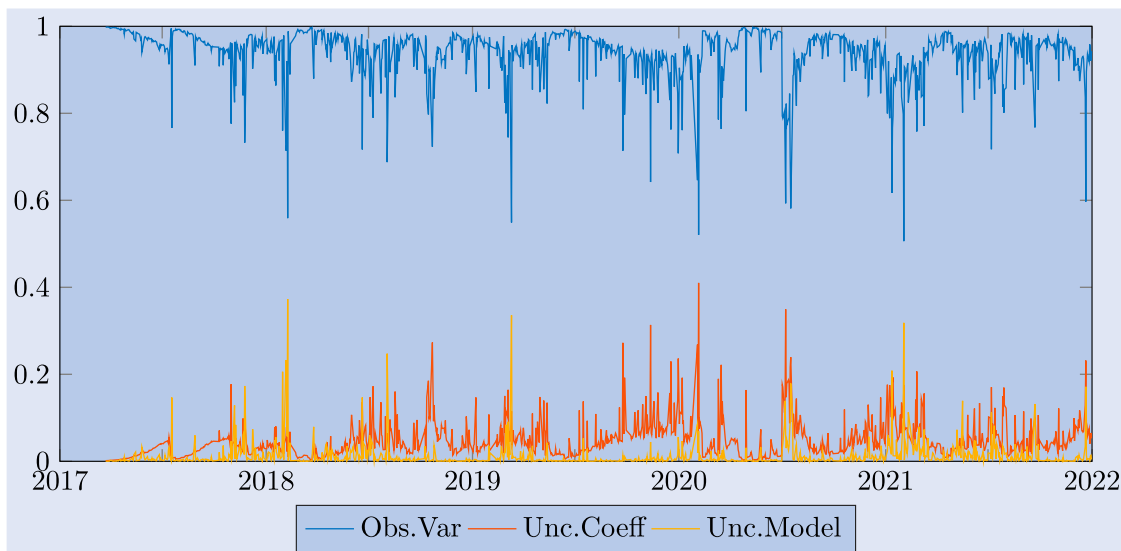


Figure 2. Weights of three components of prediction uncertainty over time.

Table 7. Out-of-sample performance in forecasting realized variance for different forecast horizon.

	$h = 5$		$h = 10$		$h = 22$	
	Loss $\times 10^8$	MCS	Loss $\times 10^4$	MCS	Loss	MCS
HAR	0.200	(0.256)	0.201	(0.357)	0.201	(0.001)
CV	0.203	(0.311)	0.202	(0.514)	0.197	(0.006)
DMA(0.99)	0.186*	(1.000)	0.172	(0.669)	0.150	(0.047)
DMS(0.99)	0.193	(0.311)	0.176	(0.669)	0.153	(0.019)
DMA(0.95)	0.217	(0.255)	0.165*	(1.000)	0.118*	(1.000)
DMS(0.95)	0.225	(0.155)	0.171	(0.669)	0.129	(0.156)
BMA	0.187	(0.985)	0.176	(0.669)	0.164	(0.002)
BMS	0.186	(0.985)	0.175	(0.669)	0.165	(0.003)
MC	0.220	(0.225)	0.172	(0.669)	0.118	(0.606)
TMC	0.220	(0.227)	0.172	(0.669)	0.118	(0.606)
DMSPE(0.9)	0.221	(0.161)	0.173	(0.669)	0.118	(0.464)
DMSPE(1.0)	0.220	(0.230)	0.172	(0.669)	0.118	(0.904)

Note: This table provides the forecasting performance of DPCFM and its competing strategies in forecasting next week RV. The number in bold denote that the corresponding model has the lowest loss function under a specific criterion. * denotes that the corresponding model has the highest MCS p -value.

For a comparison, we choose three models that perform well in Bollerslev *et al.* (2022): the vech-HAR, vech-HAR-RS, and vech-PCOV(2) models. The vech-HAR model is the traditional covariance-forecasting model, the vech-HAR-RS model uses zero as the threshold, and the vech-PCOV(2) model adds an additional threshold of 0.1 to the vech-HAR-RS model.

Table 8 reports the out-of-sample forecasting performances of five different forecasting models. From the table, the following are worthy of note: First, DMA(0.99) generates substantially lower forecasting errors than the other four models in all four dimensions and three forecasting periods. More specifically, in terms of 1-day-ahead forecasts, the average RMSE for the three vech-HAR models is approximately 25.36, while the value for the DM(0.99) is 24.77, with MCS p -value equals 1. This evidence suggests that the DMA(0.99) has higher accuracy in forecasting the RCOV matrix than the vech-HAR model. Also, we observe a similar pattern for the weekly and monthly forecasting performances compared with the daily forecasting results. Specifically, the average weekly and monthly forecasting errors for the vech-HAR models are 17.33 and 15.54, respectively. However, the average weekly and monthly RMSEs for the DMA(0.99) are merely 15.96 and 13.40, respectively. This result indicates that as prediction horizons increase, the DMA method can achieve better forecasting performance than the vech-HAR models, thereby

highlighting the importance of incorporating the TVPs of predictors and forecasting models in the prediction of future RCOV.

5.2. Portfolio selection

In this subsection, we examine the economic value of the DPCFM in this study from a portfolio-selection perspective. Consider a risk-averse investor who allocates their funds into N risky assets based on the forecasts for the daily covariance matrix of the returns on an asset, Σ_t . The investor solves the GMVP problem:

$$w_t = \underset{w_t}{\operatorname{argmin}} w_t' \Sigma_t w_t, \quad \text{st. } w_t' l = 1. \quad (20)$$

where l is an $N \times 1$ vector of ones, and w_t denotes the portfolio weight. Using the GMVP strategy, we can obtain the portfolio weight for each forecasting method through its RCOV forecasts. We then use the given portfolio weight and actual covariance to measure the actual portfolio variance.

To ensure the positive-definiteness of the $\hat{\Sigma}_t$ that is forecasted by the DPCFM, we follow Hautsch *et al.* (2012) and apply eigenvalue cleaning to every matrix that has eigenvalues smaller than or equal to 0. Eigenvalue cleaning approach replaces the negative eigenvalues with the minimum positive eigenvalue, more details can be found in Hautsch *et al.* (2012).

Table 8. Out-of-sample performance in forecasting realized covariance matrices.

	$h = 1$		$h = 5$		$h = 22$	
	RMSE	MCS	RMSE	MCS	RMSE	MCS
vech-HAR	25.364	(0.000)	17.332	(0.000)	15.540	(0.000)
vech-HAR-RS	25.153	(0.000)	17.040	(0.000)	15.494	(0.000)
vech-HAR-PCOV(2)	25.091	(0.000)	17.013	(0.000)	15.567	(0.000)
DMA(0.99)	24.770*	(1.000)	15.956*	(1.000)	13.402*	(1.000)
DMS(0.99)	24.945	(0.000)	16.069	(0.000)	13.466	(0.000)

Note: This table provides the forecasting performance in forecasting realized covariance matrices of DPCFM and its competing strategies. vech-HAR-PCOV(2) represents the model choosing a zero threshold and a 0.1 threshold quantile. The number in bold denotes that the corresponding model has the lowest loss function under a specific criterion. * denotes that the corresponding model has the highest MCS p -value.

Table 9. Portfolio performance and MCS p -values.

	$h = 1$		$h = 5$		$h = 22$	
	Portfolio variance	MCS	Portfolio variance	MCS	Portfolio variance	MCS
vech-HAR	9.436	(0.021)	9.846	(0.000)	10.351	(0.004)
vech-HAR-RS	9.428	(0.276)	9.808	(0.008)	10.331	(0.004)
vech-HAR-PCOV(2)	9.506	(0.003)	9.844	(0.000)	10.391	(0.000)
DMA(0.99)	9.389*	(1.000)	9.696*	(1.000)	10.135*	(1.000)
DMS(0.99)	9.471	(0.021)	9.724	(0.033)	10.167	(0.009)

Note: This table provides the portfolio performance of DPCFM and its competing strategies. vech-HAR-PCOV(2) represents the model choosing a zero threshold and a 0.1 threshold quantile. The number in bold denotes that the corresponding model has the lowest loss function under a specific criterion. * denotes that the corresponding model has the highest MCS p -value.

Table 9 reports the actual portfolio variance and corresponding results of the MCS test. Consistent with the empirical results in table 8, the DMA(0.99) always survives in the MCS across all the forecast horizons. In terms of the weekly and monthly portfolios, DMA(0.99) obtains the largest p -value of 1, indicating its highest economic gain among all the five models. To sum up, the empirical results in table 9 suggest that we should take into account the variability of the prediction model and its parameters when forecasting RCOV.

6. Conclusion

This study incorporates the DMA method into the partial variance forecasting model proposed by Bollerslev *et al.* (2022), and proposes a dynamic partial (co)variance forecasting model. Bollerslev *et al.* (2022) uses K-fold algorithms to choose optimal thresholds, but issues like complex computation and non-time-varying thresholds occur. The incorporation of the DMA method alleviates such issues. On one hand, the use of the DMA method simplifies the computation process of selecting threshold combinations, improving the computation efficiency. On the other hand, this dynamic partial forecasting model enables the change in the number and location of thresholds over time, providing more possibility for asset managers to control portfolio risk and achieve their investment target in the long investment horizon.

Integrated with the Chinese stock market, the dynamic partial (co)variance forecasting model indeed consistently exhibits more accurate forecasts when compared with traditional HAR and individual partial (co)variance forecasting models proposed by Bollerslev *et al.* (2022), as well as several traditional combination strategies. Even when alternative estimation windows are employed, the superiority of the dynamic partial (co)variance forecasting model remains robust and pronounced. Moreover, in the realm of multivariate analyzes, the dynamic partial (co)variance forecasting model demonstrates notable predictive efficiency. Additionally, the result from the construction of the global minimum variance portfolio (GMVP) verifies robustly good forecasting performances of the dynamic partial (co)variance forecasting model from the perspective of economic values.

Disclosure statement

No potential conflict of interest was reported by the author(s).

Funding

This research did not receive any specific grant from funding agencies in the public, commercial, or not-for-profit sectors.

Supplemental data

Supplemental data for this article can be accessed online at <https://doi.org/10.1080/14697688.2024.2342896>.

Data availability statement

The data that support the findings of this study are available from Weisheng Database. Restrictions apply to the availability of these data, which were used under license for this study.

References

- Andersen, T.G. and Bollerslev, T., Answering the skeptics: Yes, standard volatility models do provide accurate forecasts. *Int. Econ. Rev. (Philadelphia)*, 1998, **39**(4), 885–905.
- Andersen, T.G., Bollerslev, T. and Diebold, F.X., Roughing it up: Including jump components in the measurement, modeling, and forecasting of return volatility. *Rev. Econ. Stat.*, 2007, **89**(4), 701–720.
- Andersen, T.G., Bollerslev, T. and Diebold, F.X., Parametric and nonparametric volatility measurement. In *Handbook of Financial Econometrics: Tools and Techniques*, edited by Yacine Ait-Sahalia and Lars Peter Hansen, pp. 67–137, 2010 (Elsevier: Amsterdam).
- Banerjee, A. and Urga, G., Modelling structural breaks, long memory and stock market volatility: An overview. *J. Econom.*, 2005, **129**(1–2), 1–34.
- Barndorff-Nielsen, O.E., Kinnebrock, S. and Shephard, N., Measuring downside risk-realised semivariance. CREATES Research Paper, (2008–42), 2008.
- Bollerslev, T., Generalized autoregressive conditional heteroskedasticity. *J. Econom.*, 1986, **31**(3), 307–327.
- Bollerslev, T., Li, J., Patton, A.J. and Quaedvlieg, R., Realized semicovariances. *Econometrica*, 2020, **88**(4), 1515–1551.
- Bollerslev, T., Medeiros, M.C., Patton, A.J. and Quaedvlieg, R., From zero to hero: Realized partial (co) variances. *J. Econom.*, 2022, **231**(2), 348–360.
- Calvet, L.E. and Fisher, A.J., How to forecast long-run volatility: Regime switching and the estimation of multifractal processes. *J. Financ. Econom.*, 2004, **2**(1), 49–83.
- Chiriac, R. and Voev, V., Modelling and forecasting multivariate realized volatility. *J. Appl. Econ.*, 2011, **26**(6), 922–947.
- Corsi, F., A simple approximate long-memory model of realized volatility. *J. Financ. Econ.*, 2009, **7**(2), 174–196.

- Corsi, F., Mittnik, S., Pigorsch, C. and Pigorsch, U., The volatility of realized volatility. *Econom. Rev.*, 2008, **27**(1-3), 46–78.
- Dangl, T. and Halling, M., Predictive regressions with time-varying coefficients. *J. Financ. Econ.*, 2012, **106**(1), 157–181.
- Diebold, F.X. and Mariano, R.S., Comparing predictive accuracy. *J. Bus. Econ. Stat.*, 1995, **13**(3), 253–263.
- Engle, R.F., Autoregressive conditional heteroscedasticity with estimates of the variance of United Kingdom inflation. *Econometrica*, 1982, **50**(4), 987–1007.
- Granger, C.W. and Hyung, N., Occasional structural breaks and long memory with an application to the S&P 500 absolute stock returns. *J. Empir. Finance*, 2004, **11**(3), 399–421.
- Hansen, P.R., Lunde, A. and Nason, J.M., The model confidence set. *Econometrica*, 2011, **79**(2), 453–497.
- Hautsch, N., Kyj, L.M. and Oomen, R.C., A blocking and regularization approach to high-dimensional realized covariance estimation. *J. Appl. Econom.*, 2012, **27**(4), 625–645.
- Kim, C.-J. and Nelson, C.R., *State-Space Models with Regime Switching: Classical and Gibbs-Sampling Approaches with Applications*, Vol. 1, 1999 (MIT Press Books: Cambridge).
- Koop, G. and Korobilis, D., Forecasting inflation using dynamic model averaging. *Int. Econ. Rev. (Philadelphia)*, 2012, **53**(3), 867–886.
- Liu, C. and Maheu, J.M., Forecasting realized volatility: A Bayesian model-averaging approach. *J. Appl. Econom.*, 2009, **24**(5), 709–733.
- Patton, A.J. and Sheppard, K., Good volatility, bad volatility: Signed jumps and the persistence of volatility. *Rev. Econ. Stat.*, 2015, **97**(3), 683–697.
- Raftery, A.E., Kárnáží, M. and Ettler, P., Online prediction under model uncertainty via dynamic model averaging: Application to a cold rolling mill. *Technometrics*, 2010, **52**(1), 52–66.
- Stock, J.H. and Watson, M.W., Forecasting output and inflation: The role of asset prices. *J. Econ. Lit.*, 2003, **41**(3), 788–829.
- Stock, J.H. and Watson, M.W., Combination forecasts of output growth in a seven-country data set. *J. Forecast.*, 2004, **23**(6), 405–430.
- Wang, Y., Ma, F., Wei, Y. and Wu, C., Forecasting realized volatility in a changing world: A dynamic model averaging approach. *J. Bank. Financ.*, 2016, **64**, 136–149.